# Intermodulation Distortion Analysis Using a Frequency-Domain Harmonic Balance Technique

JOHN H. HAYWOOD AND Y. LEONARD CHOW, MEMBER, IEEE

*Abstract*—A simple approach to the technique of harmonic balance for nonlinear circuit analysis is presented. The algorithm operates solely in the frequency domain to simplify the resolution of the intermodulation products of two input tones with narrow frequency spacing.

A description of the technique and its implementation is given. The harmonic and intermodulation products of a single FET amplifier are calculated and the results compared with a Volterra series analysis and experimentally measured values. A second single FET amplifier is analyzed to show the accuracy of the prediction of gain compression with this technique.

The accuracy of this technique is shown to equal that of the Volterra series analysis used in the comparison. The ability of the frequency-domain technique to routinely analyze arbitrary circuit topologies, however, provides a definite advantage over the Volterra series method.

## I. INTRODUCTION

PRESENT COMMERCIALLY available computer-aided nonlinear analysis techniques for microwave circuits consists wholly or partially of solution in the time domain of the differential equations describing the network. Analysis packages such as SPICE [1] and Watand [2] solve the entire system of equations simultaneously for each time step. For networks with time constants large with respect to one problem of the driving signal, this time-domain solution may have to be performed over many full periods of the input waveform until the system has reached steady state.

Nakhla and Vlach [3] have modified the harmonic balance technique of Bailey [4] and Lindenlaub [5] to minimize the number of differential equations to be solved. In this case, the network is split into linear and nonlinear subnetworks, the linear subnetwork containing only linear elements and the nonlinear subnetwork containing all of the nonlinear elements and possibly some linear elements for convenience. The linear subnetwork is solved in the frequency domain, leaving only the nonlinear subnetwork to be solved in the time domain. The discrete Fourier transform is employed to convert the resulting waveform into its frequency spectrum. The harmonic balance technique is used to match the harmonic amplitudes of current or voltage in the set of branches joining the linear and nonlinear subnetworks.

Manuscript received August 27, 1987; revised March 17, 1988. This work was supported by the National Science and Engineering Research Council and the Communications Research Centre.

The authors are with the Department of Electrical Engineering, University of Waterloo, Waterloo, Ontario, Canada N2L 3G1.

IEEE Log Number 8821758.

The above techniques are very successful for systems with a single driving frequency since the number of time samples required to resolve the spectral amplitudes of the harmonically related branch currents and voltages is determined by the Nyquist criterion. Therefore, to determine the amplitude of harmonics of order $N_h$ requires only $2 \cdot N_h + 1$ time samples.

To determine the intermodulation products of a network with two driving frequencies, however, requires the resolution of the amplitudes of nonharmonically related branch currents and voltages. The required number of time samples increases as the reciprocal of the input frequency spacing and can become prohibitively large.

Gilmore [6] uses a bandpass sampling technique to reduce the number of time samples required. By sampling at the bandpass rate as opposed to the higher Nyquist rate, the fundamentals and surrounding odd-order intermodulation products are aliased with the lower frequency, even-order intermodulation products. This aliasing requires that an input frequency shift and time domain solution be performed to extract the current and voltage amplitudes at each frequency.

One analytical technique exists which is able to predict the harmonic and intermodulation products of nonlinear circuits. The Volterra series relates the output $v(t)$ to the input $x(t)$ by a series of convolutions in the time domain:

$$\begin{aligned} v(t) = &\int_{-\infty}^{+\infty} h_1(\tau) x(t-\tau)\, d\tau \\ &+ \int_{-\infty}^{+\infty}\int_{-\infty}^{+\infty} h_2(\tau_1,\tau_2) x(t-\tau_1) x(t-\tau_2)\, d\tau_1 d\tau_2 \\ &+ \int_{-\infty}^{+\infty}\int_{-\infty}^{+\infty}\int_{-\infty}^{+\infty} h_3(\tau_1,\tau_2,\tau_3) x(t-\tau_1) \\ &\cdot x(t-\tau_2) x(t-\tau_3)\, d\tau_1 d\tau_2 d\tau_3 + \cdots . \end{aligned} \tag{1}$$

The $h_n(\tau_1,\cdots,\tau_n)$ are the $n$-dimensional impulse responses characterizing the system. They are derived from the circuit topology and component values by a rigorous, algebraic technique [7], [8]. The Volterra series is a powerful technique for analyzing circuits with a fixed topology, as truncation of the infinite series is the only source of error. The nonlinear impulse responses must be derived for each different circuit topology, however, making this technique impractical for computer-aided analysis of arbitrary structures.

This paper introduces a harmonic balance technique in the frequency domain for efficiently determining the harmonic and intermodulation products of nonlinear networks with multitone inputs. This eliminates the solution of the system equations in the time domain, conversion from the time domain to the frequency domain (discrete Fourier transform), and reconstruction of the port voltage time-domain waveforms from their Fourier series coefficients.

The concept of a harmonic balance operating solely in the frequency domain has been exploited previously by Rhyne and Steer [9], [10]. Their technique is based on a formula developed by Steer and Khan [11] which predicts the output current spectrum of a nonlinearity with a multitone input, when the nonlinear $I/V$ characteristic is a power series dependent on a single voltage with complex coefficients and frequency-dependent time delays.

In this paper we have chosen to represent the nonlinearities by a simple power series relating the element's magnitude to its terminal voltage. The element's current spectrum may now be determined by a series of convolutions in the frequency domain and possibly a differential or integration (multiplication or division by $j\omega$) in the case of a nonlinear capacitor or inductor, respectively. Although both the approach of this paper and that of Rhyne and Steer are based on operations in the frequency domain, the simplicity of the convolution of discrete frequency spectra renders the technique of this paper much simpler and more straightforward.

Theoretically, this technique could be used for any magnitude of nonlinearity. Large nonlinearities, however, would require a greater number of terms in the power series expansion and more harmonics and intermodulation products to accurately represent the current and voltage waveforms. In this paper we will consider both small and moderate nonlinearities, those which can be accurately represented by four power series coefficients, and harmonic and intermodulation products up to seventh and third order, respectively.

A complete description of the technique is given in the following section. A successful method for optimizing the matrix of linear–nonlinear interface port currents to obtain the minimum error is discussed in Section III. A simple single-stage FET amplifier as studied by Minasian [12] is used as an example to demonstrate the ability of this technique to predict intermodulation distortions. A second example, based on a FET amplifier as studied by Law *et al.* [13], illustrates the accuracy of the prediction of gain saturation. The results of these examples are compared with their respective Volterra series analyses and experimental results.

## II. Description of Frequency-Domain Technique

The harmonic balance technique of Nakhla and Vlach [3] requires that the network to be analyzed be split up into a strictly linear subnetwork, for analysis in the frequency domain, and a nonlinear subnetwork, possibly

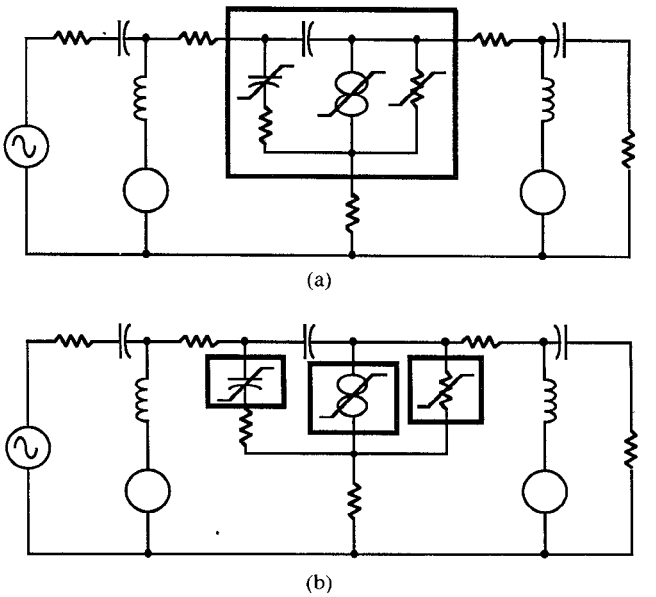


Fig. 1. Division of network into linear and nonlinear subnetworks. (a) Standard harmonic balance technique. (b) Frequency-domain harmonic balance technique.

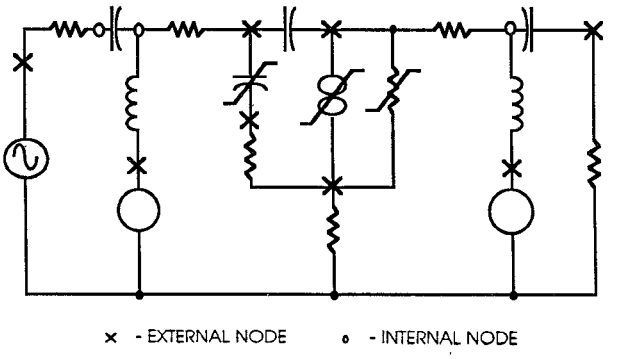


Fig. 2. Internal/external node division.

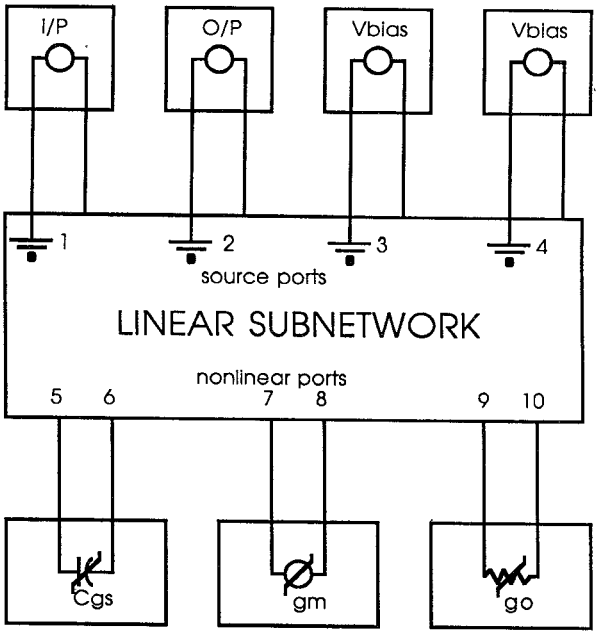


Fig. 3. Source port and nonlinear port connections to linear subnetwork.

including some linear elements for convenience, for analysis in the time domain.

In the frequency-domain harmonic balance technique (FDHB) of this paper, the network is divided into a linear subnetwork encompassing ***all*** of the linear elements, and a series of nonlinear subnetworks, each comprising only a single nonlinear element (Fig. 1). Given the input frequencies and the orders of the harmonic and intermodulation products to be determined, a vector of the pertinent frequencies can be constructed. A nodal admittance matrix is calculated for the linear subnetwork at each frequency. The network nodes are divided into two types: external nodes, to which voltage sources or nonlinear elements are connected, and internal nodes, which are connected only to other linear elements (Fig. 2). The nodal admittance matrix is thus

$$\begin{pmatrix} [Y_{ee}] & [Y_{ei}] \\ [Y_{ie}] & [Y_{ii}] \end{pmatrix} \begin{pmatrix} \begin{pmatrix} V_{EX_1} \\ V_{EX_2} \\ \vdots \\ V_{EX_{nex}} \end{pmatrix} \\ \begin{pmatrix} V_{IN_1} \\ V_{IN_2} \\ \vdots \\ V_{IN_{nin}} \end{pmatrix} \end{pmatrix} = \begin{pmatrix} \begin{pmatrix} I_{EX_1} \\ I_{EX_2} \\ \vdots \\ I_{EX_{nex}} \end{pmatrix} \\ \begin{pmatrix} 0 \\ 0 \\ \vdots \\ 0 \end{pmatrix} \end{pmatrix}. \quad (2)$$

By solving for the internal node voltages, $[V_{IN}]$, in terms of external node voltages, $[V_{EX}]$, the reduced nodal admittance matrix, $[Y_{\text{red}}]$, can be constructed, which relates external node currents only to external node voltages. The internal voltages are expressed in terms of external voltages as follows:

$$[V_{IN}] = [Y_{ii}]^{-1}[Y_{ei}][V_{EX}]. \quad (3)$$

Using this to eliminate $[V_{IN}]$ from (2), we obtain

$$[Y_{\text{red}}][V_{EX}] = \left[[Y_{ee}] + [Y_{ei}][Y_{ii}]^{-1}[Y_{ie}]\right][V_{EX}] = [I_{EX}]. \quad (4)$$

This reduced matrix can be considered to be a port admittance matrix, with all port voltages being with respect to the network ground. This preprocessing of the nodal admittance matrix has two advantages:

1) the addition of linear subnetwork nodes and branches does not increase the size of the problem once the reduced admittance matrix has been constructed;
2) only the external node voltages are calculated at each iteration, thereby increasing the iteration rate.

The external nodes (ports) are divided into two types: ***source*** ports (input, output, and dc bias connections) and ***nonlinear*** ports, to which the nonlinear elements are connected (Fig. 3).

With the nonlinear elements isolated, the constitutive relations for each of the nonlinear subnetworks can be written analytically in a power series form dependent on their terminal voltages. As an example, consider a nonlinear conductance:

$$i(t) = g_0 + g_1 \cdot v(t) + g_2 \cdot v^2(t) + g_3 \cdot v^3(t) + \cdots \quad (5)$$

where $v(t)$ is the real-valued time-domain terminal voltage waveform. Using the Fourier transform, the current spectrum can be written:

$$I(\omega) = g_0 \cdot \delta(\omega) + g_1 \cdot V(\omega) + g_2 \cdot V(\omega) * V(\omega) + g_3 \cdot V(\omega) * V(\omega) * V(\omega) + \cdots \quad (6)$$

where $\delta(\omega)$ is a Dirac delta function, and * denotes convolution. Similarly, for a capacitor,

$$i(t) = \frac{d}{dt}\left(C_0 \cdot v(t) + C_1 \cdot v^2(t) + C_2 \cdot v^3(t) + \cdots\right) \quad (7)$$

and

$$I(\omega) = j\omega\left(C_0 \cdot V(\omega) + C_1 \cdot V(\omega) * V(\omega) + C_2 \cdot V(\omega) * V(\omega) * V(\omega) + \cdots\right). \quad (8)$$

Now the current spectrum of the nonlinear subnetworks can be determined directly from the applied voltage spectrum. In this manner we eliminate the need for reconstructing the terminal voltage waveform and subsequent DFT. By performing all calculations in the frequency domain, resolving the intermodulation products of two narrowly spaced input frequencies ceases to be a problem. The algorithm used for this technique is shown below:

1) Construct the vector of $N_f$ frequencies, $f_k$, $1 \leqslant k \leqslant N_f$, to be used in the analysis.
2) Construct the linear port admittance matrix at each frequency.
3) Establish the initial guesses for the currents $I^i_{L_{k,p}}$ at each port, $p$, and each frequency, $f_k$. The simplest choice of these is the set of currents which exists when all nonlinear elements are replaced by their linear equivalents.
4) Apply these currents to the linear port admittance matrix to determine the nonlinear port voltages, $V^i_{L_{k,p}}$.
5) For each nonlinear element, determine, by convolutions, the nonlinear element currents, $I^i_{NL_{k,p}}$.
6) Using a suitable optimization method, choose a new set of nonlinear port currents, $I^{i+1}_{L_{k,p}}$, to minimize the error between the chosen nonlinear port currents, $I^{i+1}_{L_{k,p}}$, and the computed nonlinear element currents, $I^{i+1}_{NL_{k,p}}$.
7) Iterate 4 to 6 until a predetermined error threshold is reached.

To obtain the nonlinear port voltages from the port currents in step 4, the linear port admittance matrix is divided into four submatrices:

$$\begin{pmatrix} [A] & [B] \\ [C] & [D] \end{pmatrix} \begin{pmatrix} \begin{pmatrix} V_{\text{source}_1} \\ V_{\text{source}_2} \\ \vdots \\ V_{\text{source}_{ns}} \end{pmatrix} \\ \begin{pmatrix} V_{L_1} \\ V_{L_2} \\ \vdots \\ V_{L_{nnl}} \end{pmatrix} \end{pmatrix} = \begin{pmatrix} \begin{pmatrix} I_{\text{source}_1} \\ I_{\text{source}_2} \\ \vdots \\ I_{\text{source}_{ns}} \end{pmatrix} \\ \begin{pmatrix} I_{L_1} \\ I_{L_2} \\ \vdots \\ I_{L_{nnl}} \end{pmatrix} \end{pmatrix}. \quad (9)$$

Submatrix $A$ relates the source port currents to the source port voltages. Submatrix $B$ relates the source port currents to the nonlinear port voltages. Submatrices $C$ and $D$ relate the nonlinear port currents to the source port voltages and nonlinear port voltages, respectively. The nonlinear port voltages can now be obtained from

$$\begin{pmatrix} V_{L_1} \\ V_{L_2} \\ \vdots \\ V_{L_{nnl}} \end{pmatrix} = [D]^{-1} \left( \begin{pmatrix} I_{L_1} \\ I_{L_2} \\ \vdots \\ I_{L_{nnl}} \end{pmatrix} - [C] \begin{pmatrix} V_{\text{source}_1} \\ V_{\text{source}_2} \\ \vdots \\ V_{\text{source}_{nnl}} \end{pmatrix} \right). \quad (10)$$

This process is repeated for each frequency, $f_k$.

The nonlinear port currents are then found in step 5 using equations similar to (6) above. Since the port voltage and current spectra consist of a series of complex-valued delta functions rather than continuous spectra, the convolutions can be computed exactly and are a simple matter of a frequency shift and a sum of the products of complex numbers for each frequency component.

## III. Optimization

The objective of the optimization routine is to predict a matrix of complex nonlinear port currents which will minimize the error between these currents, which are applied to the linear subnetwork, and the currents obtained from the nonlinear elements. The definition of error at the $i$th iteration is

$$\text{error}_i = \sum_{p=1}^{N_p} \sum_{k=1}^{N_f} \frac{|I^i_{L_{k,p}} - I^i_{NL_{k,p}}|^2}{|I^i_{L_{1,p}}|^2}. \quad (11)$$

This is the same definition as that used by Gilmore [6], with the exception that the error at each port is now normalized to the square of the amplitude of the fundamental at that port. This ensures that the current at each port contributes equally to the total error, and each will be of equal importance in the optimization.

The major obstacles to the optimization were the large number of variables to be optimized and the inability to determine the gradient of the error with respect to these variables.

A technique which does not require gradients is used by Hicks and Khan [14]. A type of relaxation method, this technique predicts a matrix of nonlinear port currents, $I^{i+1}_{L_{k,p}}$, for the $i+1$ iteration which is a weighted average of the previous iteration's nonlinear port currents, $I^i_{L_{k,p}}$, and nonlinear element currents, $I^i_{NL_{k,p}}$:

$$I^{i+1}_{L_{k,p}} = \lambda \cdot I^i_{NL_{k,p}} + (1-\lambda) \cdot I^i_{L_{k,p}}, \qquad 0 \leqslant \lambda \leqslant 1. \quad (12)$$

This eliminates optimization with respect to each of a large number of variables, as in the case of a gradient or direct search method. The value of the error at each iteration, however, is used only as a measure of the accuracy of the result. The optimization method employed with the FDHB method of this paper chooses an optimum value for the weighting factor $\lambda$ based on the variation of the error at each iteration.

The nonlinear port current matrix consists of complex numbers representing the current at each of $N_p$ nonlinear ports and $N_f$ frequencies of interest. This matrix can be considered to describe a point in complex $N$ space, where

$$N = N_f \cdot N_p. \quad (13)$$

Assuming, as before, that a superior estimate of the true nonlinear port currents exists along a line joining the points $I^i_{L_{k,p}}$ and $I^i_{NL_{k,p}}$ in $N$ space, it remains to search along this line for an optimum value for $\lambda$ to minimize the error. The algorithm used is as follows:

1) Use $I^i_{L_{k,p}}$ to calculate $I^i_{NL_{k,p}}$ and the error. This error corresponds to $\lambda = 0$.
2) Calculate the error using $I^{i\prime}_{L_{k,p}} = (I^i_{L_{k,p}} + I^i_{NL_{k,p}})/2$. This error corresponds to $\lambda = 0.5$.
3) Calculate the error using $I^{i\prime\prime}_{L_{k,p}} = I^i_{NL_{k,p}}$, $(\lambda = 1)$.
4) Choose an optimum $\lambda, \lambda_O$, by finding the minimum of a parabola fitting the three $(\lambda, \textit{error})$ points.
5) Calculate the new $I^{i+1}_{L_{k,p}} = \lambda_O \cdot I^i_{NL_{k,p}} + (1-\lambda_O) \cdot I^i_{L_{k,p}}$.

The success of this method is illustrated in the following section.

## IV. Results

Two examples are given here. The first is an example of the prediction of intermodulation products arising from a small nonlinearity. The circuit is one previously studied by Minasian [12]. This choice was made since all nonlinear coefficients and component values are tabulated in [12], allowing a direct comparison of the Volterra series analysis and experimental results with the results of the FDHB technique of this paper. The circuit and nonlinear coefficients are shown in Fig. 4. The fundamental and third-order intermodulation products were calculated with an input consisting of two tones with a center frequency of 2.4 GHz and a frequency spacing of 2 MHz at six different power levels. These values are plotted in Fig. 5. The error threshold used for the FDHB results was $1.0 \times 10^{-10}$. The maximum discrepancy between the nonlinear port currents and the nonlinear element currents at any port and any frequency is therefore 100 dB below the magnitude of the fundamental at that port. Also shown in Fig. 5 for comparison are experimentally measured values and Volterra series predictions of Minasian. The Volterra series is an analytical technique which, when given exact nonlinear coefficients, should yield theoretically exact results. The analysis by Minasian includes two simplifying assumptions:

1) the source impedance at the difference frequency, $f_1 - f_2$, is small compared to the input impedance of the FET;
2) the contribution to the power at $2f_1 - f_2$ by intermodulations above third order is negligible.

Inspection of Fig. 5 reveals that the accuracy of the FDHB results is equal that of the Volterra series analysis. Whereas Minasian used a closed-form expression to characterize the output conductance, $g_o$, the FDHB technique

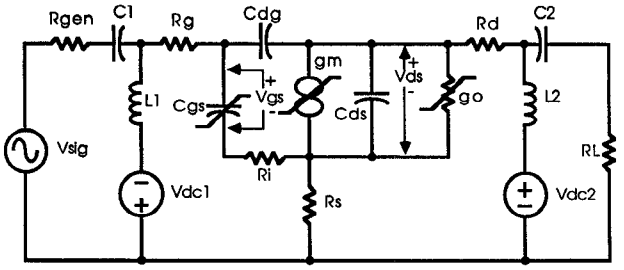


| | | | | | |
|---|---|---|---|---|---|
| Vdc1 | = | 0.0 V | Vdc2 | = | 3.5 V |
| Rgen | = | 50.0 Ω | C2 | = | 10 nF |
| C1 | = | 10 nF | L2 | = | 10 μH |
| L1 | = | 10 μH | Rs | = | 1 mΩ |
| Rg | = | 1 mΩ | Ri | = | 45.0 Ω |
| Rd | = | 1 mΩ | Cdg | = | 0.088 pF |
| Cds | = | 0.067 pF | | | |

$Cgs(vgs) = .364 + .082\ vgs$ pF

$gm(vgs) = .012 + .0024\ vgs - .0016\ vgs^2$ S

$go(vgs) = 73.92 * 10^{-6} - 19.85 * 10^{-6} vds + 11.0 * 10^{-6} vds^2$ S

Fig. 4. Single FET amplifier and component values of first example.

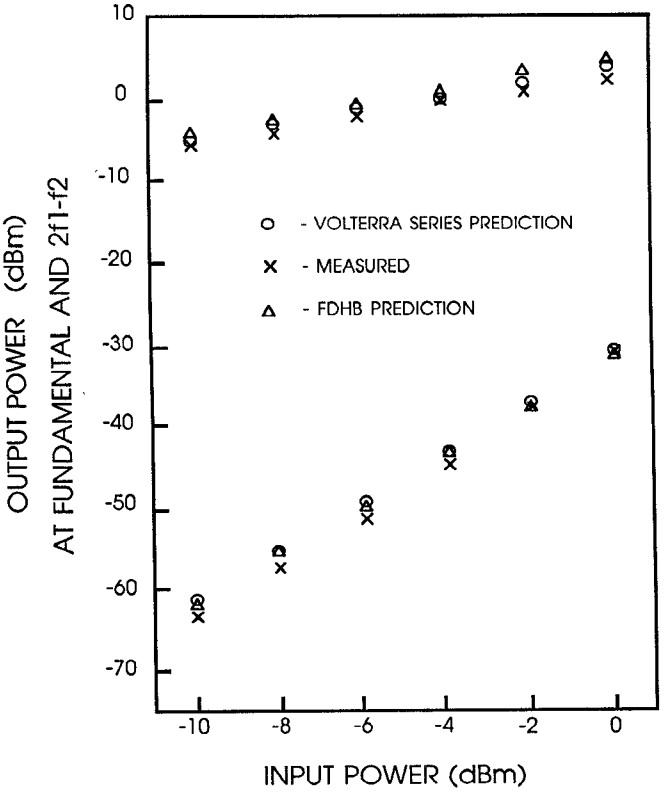


Fig. 5. Measured and predicted fundamental and third-order intermodulation distortion power versus available input power. Center frequency = 2.4 GHz.

dictated the use of a power series representation. This, or the assumptions made by Minasian in his analysis, may serve to explain the small discrepancy in results between the two techniques.

The second example demonstrates the prediction of gain compression as the nonlinearity is increased by an increase in the input power level. The circuit analyzed, shown in Fig. 6, is one previously studied by Law and Aitchison

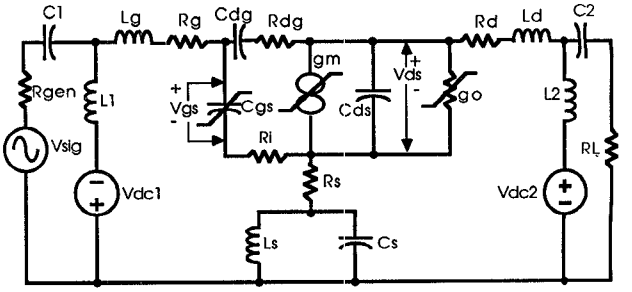


| | | | | | |
|---|---|---|---|---|---|
| Vdc1 | = | -1.0 V | Vdc2 | = | 8.0 V |
| Lg | = | 0.46 nH | Cdg | = | 0.021 pF |
| Rg | = | 0.5 Ω | Rdg | = | 29.0 Ω |
| Ri | = | 5.4 Ω | Cds | = | 0.06 pF |
| Rs | = | 2.0 Ω | Rd | = | 3.0 Ω |
| Ls | = | 0.1 nH | Ld | = | 0.5 nH |
| Cs | = | 0.15 pF | C1 | = | 10.0 nF |
| C2 | = | 10.0 nF | L1 | = | 10.0 μH |
| L2 | = | 10.0 μH | RL | = | 50.0 Ω |
| Rgen | = | 50.0 Ω | | | |

$Cgs(vgs) = 0.55 + 0.2\ vgs + 0.06\ vgs^2$ pF

$gm(vgs) = 36.5 + 2.4\ vgs - 1.0\ vgs^2$ mS

$go(vds) = 1.8 - 0.2\ vds + 0.02\ vds^2$ mS

Fig. 6. Single FET amplifier and component values of second example.

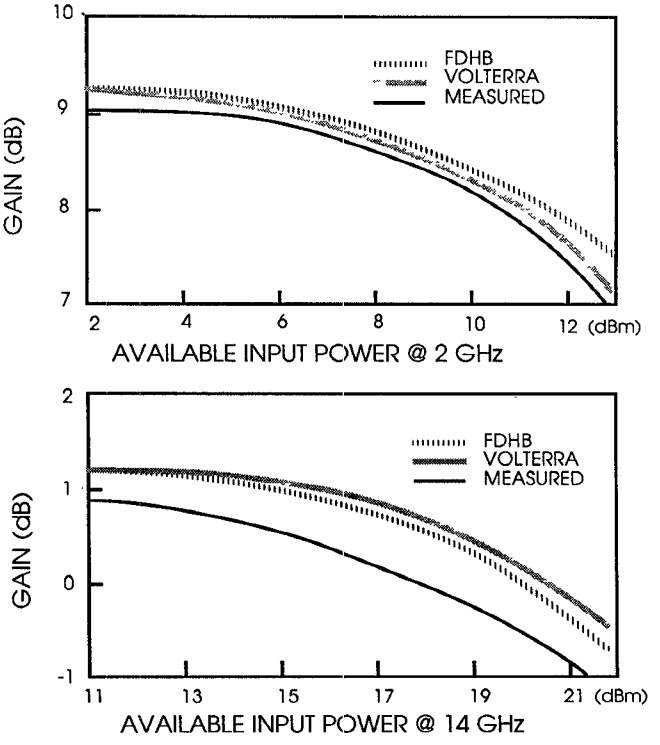


Fig. 7. Power gain versus available input power for second example.

[13]. The power gain of the circuit was computed over a 14 dB range of available input power at 2 and 14 GHz to demonstrate the capability of the FDHB technique to predict gain saturation. Again, excellent agreement is obtained between the FDHB predictions and the measured values and Volterra series predictions of Law and Aitchison shown in Fig. 7.

To determine the effect of including more harmonics in the calculations, a series of results were generated using

TABLE I
OUTPUT POWER (DBM) AT ALL FREQUENCIES VERSUS HARMONIC ORDER (INPUT FREQUENCY, 14.0 GHZ; INPUT POWER, 8 DBM)

Output power (dBm) at all freq. vs harmonic order

Input frequency is 14.0 GHz, Input power is 8 dBm

| Frequency | Harmonic Order | | |
|---|---|---|---|
| | 5 | 6 | 7 |
| f1 | 9.341 | 9.341 | 9.341 |
| 2f1 | -16.82 | -16.82 | -16.82 |
| 3f1 | -51.71 | -51.71 | -51.71 |
| 4f1 | -73.65 | -73.64 | -73.64 |
| 5f1 | -85.58 | -85.40 | -85.40 |
| 6f1 | | -103.3 | -103.2 |
| 7f1 | | | -122.5 |

TABLE II
OUTPUT POWER (DBM) AT ALL FREQUENCIES VERSUS HARMONIC ORDER (INPUT FREQUENCY, 14.0 GHZ; INPUT POWER, 22 DBM)

Output power (dBm) at all freq. vs harmonic order

Input frequency is 14.0 GHz, Input power is 22 dBm

| Frequency | Harmonic Order | | |
|---|---|---|---|
| | 5 | 6 | 7 |
| f1 | 21.33 | 21.32 | 21.32 |
| 2f1 | 2.754 | 2.738 | 2.723 |
| 3f1 | -27.10 | -27.43 | -27.23 |
| 4f1 | -14.65 | -15.23 | -15.16 |
| 5f1 | -26.62 | -27.75 | -28.09 |
| 6f1 | | -47.57 | -52.49 |
| 7f1 | | | -46.95 |

the circuit of Fig. 6 at 14 GHz and 8 dBm available input power using harmonic orders ranging from 5 to 7. The output power at $R_L$ at each frequency is shown in Table I. In Table I it may be noted that the addition of more harmonics to the balance does not significantly change the values of the previously calculated harmonics. This is because the added harmonics have very little power relative to the others. It is expected, however, that for a case where the power in an added harmonic is closer to the powers of the previously calculated harmonics, the effect

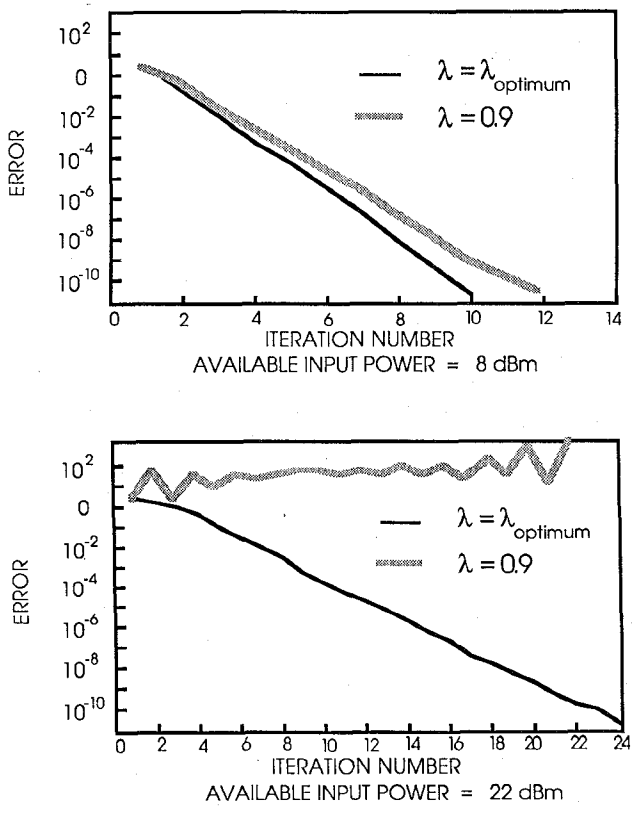


Fig. 8. Convergence rate of second example for two input power levels. Frequency = 14 GHz.

will be noticeable. To test this prediction, the input power was raised by 14 dB to 22 dBm, a fivefold increase in voltage amplitude. This enlarges the effect of the nonlinearities and increases the power in the higher harmonics, as observed in Table II. The effect of more harmonics in the computation is now noticeable.

The success of the optimization method is illustrated using the circuit of Fig. 6 operated at a frequency of 14 GHz. The error at each iteration is plotted in Fig. 8 for two different input power levels using both the Hicks–Khan fixed point method ($\lambda = 0.9$) and the method of this paper. The use of the estimated optimum weighting factor, $\lambda_O$, for each iteration resulted in a rapid and stable convergence in both cases.

At very high input power levels, the convergence may not be as stable. Cases of this type have been avoided since such extreme gain compression would never be encountered in the operation of amplifiers similar to that of Fig. 4 or Fig. 6.

## V. CONCLUSIONS

A harmonic balance technique has been presented which permits the determination of the harmonic and intermodulation distortion of nonlinear networks with single- and two-tone inputs. Representation of the nonlinearities by a power series expansion allows all computations to be performed in the frequency domain. The advantages of this method are:

1) frequency to time domain and time to frequency domain conversions are not required;

2) time-domain integration is replaced by convolution, the simplicity of which is not affected by the input frequency spacing.

The execution speed of this algorithm, therefore, is very fast. Solution of the single FET amplifier of Fig. 6, with sixth-order harmonics at a frequency of 14 GHz and an input power level of 22 dBm required 23 iterations and 1.8 seconds of CPU time on an IBM 4381. The simple representation of the nonlinearities in a power series form also enables the extension of the FDHB technique to include two-dimensional nonlinearities, for example, an output conductance dependent on both $V_{ds}$ and $V_{gs}$. Disadvantages of this technique are:

1) preprocessing of the network admittance matrix is required to separate all nonlinear elements from the linear subcircuit;
2) larger nonlinearities require more power series coefficients and correspondingly greater execution time.

In principle this technique can be applied to circuits with large nonlinearities; however, this has not been tested as there are few such examples in the literature for comparison.

The accuracy of the FDHB technique is shown to equal that of the Volterra series. The ability of the FDHB technique to routinely analyze arbitrary circuit topologies provides a distinct advantage over the Volterra series method.

## Acknowledgment

The authors would like to thank D. J. Roulston for his valuable suggestions and encouragement.

## References

[1] L. W. Nagel, "SPICE2: A computer program to simulate semiconductor circuits," Electron. Res. Lab., Univ. California, Berkeley, Memo ERL-M520, 1975.
[2] I. N. Hajj, D. J. Roulston, and P. R. Bryant, "Generation of transient response of nonlinear bipolar transistor circuits from device fabrication data," *IEEE J. Solid-State Circuits*, vol. SC-12, pp. 29–38, Feb. 1977.
[3] M. S. Nakhla and J. Vlach, "A piecewise harmonic balance technique for determination of periodic response of nonlinear systems," *IEEE Trans. Circuits Syst.*, vol. CAS-23, Feb. 1976.
[4] E. M. Bailey, "Steady state harmonic analysis of nonlinear networks," Ph.D. dissertation, Stanford Univ., Stanford, CA, 1968.
[5] J. C. Lindenlaub, "An approach for finding the sinusoidal steady state response of nonlinear systems," in *Proc. 7th Ann. Allerton Conf. Circuit and System Theory* (Univ. Illinois, Chicago), 1969.
[6] R. Gilmore, "Nonlinear circuit design using the modified harmonic balance algorithm," *IEEE Trans. Microwave Theory Tech.*, vol. MTT-34, pp. 1294–1306, Dec. 1986.
[7] E. Bedrosian and S. O. Rice, "The output properties of Volterra systems (nonlinear systems with memory) driven by harmonic and Gaussian inputs," *Proc. IEEE*, vol. 59, pp. 1688–1707, Dec. 1971.
[8] J. J. Bussgang, L. Ehrman, and J. W. Graham, "Analysis of nonlinear systems with multiple inputs," *Proc. IEEE*, vol. 62, pp. 1088–1119, Aug. 1974.
[9] G. W. Rhyne and M. B. Steer, "A new frequency domain approach to the analysis of nonlinear microwave circuits," in *IEEE MTT-S Int. Microwave Symp. Dig.*, 1985, pp. 401–404.
[10] G. W. Rhyne and M. B. Steer, "Simulation of intermodulation distortion in MESFET circuits with arbitrary frequency separation of tones," in *IEEE MTT-S Int. Microwave Symp. Dig.*, 1986, pp. 547–550.
[11] M. B. Steer and P. J. Khan, "An algebraic formula for the complex output of a system with multi-frequency excitation," *Proc. IEEE*, pp. 177–179, Jan. 1983.
[12] R. A. Minasian, "Intermodulation distortion analysis of MESFET amplifiers using the Volterra series representation," *IEEE Trans. Microwave Theory Tech.*, vol. MTT-28, pp. 1–8, Jan. 1980.
[13] C. L. Law and C. S. Aitchison, "Prediction of wide-band power performance of MESFET distributed amplifiers using the Volterra series representation," *IEEE Trans. Microwave Theory Tech.*, vol. MTT-34, pp. 1308–1317, Dec. 1986.
[14] R. G. Hicks and P. J. Khan, "Numerical analysis of nonlinear solid-state device excitation in microwave circuits," *IEEE Trans. Microwave Theory Tech.*, vol. MTT-30, pp. 251–259, Mar. 1982.

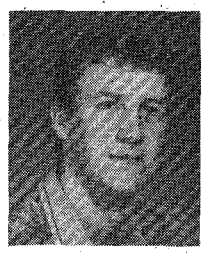

**John H. Haywood** was born in London, Ontario, Canada, on August 20, 1963. He received the B.A.Sc. degree in electrical engineering from the University of Waterloo, Ontario, Canada, in 1986. Since 1986 he has been a research and teaching assistant at the University of Waterloo and is currently completing the M.A.Sc. degree in electrical engineering. His current research interests are in the analysis of nonlinear microwave integrated circuits.

**Y. Leonard Chow** (M'60) received the Ph.D. degree from the University of Toronto, Toronto, Ontario, Canada, in 1965.

From 1964 to 1966, he worked for the National Radio Astronomy Observatory, Charlottesville, VA. As a consequence in 1974 he designed the configuration for VLA. The VLA is a "very large antenna array" comprising 27 85-ft reflectors at Socorro, NM. In 1966 he joined the University of Waterloo, Waterloo, Ontario, Canada, and became a professor in the Department of Electrical Engineering. Presently his research deals with the numerical simulation of field effects. The field effects range from high-voltage dc fields to antennas, and to fields for microwave integrated circuits, linear and nonlinear. In the microwave integrated circuit area, he is a consultant to both the Communications Research Centre, Canada, and EEsof, Inc., California.